Molecular Phylogenetics and Evolution 145 (2020) 106723

Contents lists available at ScienceDirect

Molecular Phylogenetics and Evolution

journal homepage: www.elsevier.com/locate/ympev

The roles of vicariance and dispersal in the differentiation of two species of the *Rhinella marina* species complex

Adam Bessa-Silva[a,b], Marcelo Vallinoto[a,b,*], Iracilda Sampaio[a], Oscar A. Flores-Villela[c], Eric N. Smith[d,e], Fernando Sequeira[b]

[a] Laboratório de Evolução (LEVO), Instituto de Estudos Costeiros (IECOS), Universidade Federal do Pará, Campus de Bragança, 68 600-000 Pará, Brazil
[b] CIBIO-InBIO, Centro de Investigação em Biodiversidade e Recursos Genéticos, InBIO Laboratório Associado, Campus Agrário de Vairão, Universidade do Porto, 4485–661 Vairão, Portugal
[c] Museo de Zoología, Department of Evolutionary Biology, Facultad de Ciencias, Universidad Nacional Autónoma de México, External Circuit of Ciudad Universitaria, Mexico City 04510, Mexico
[d] Department of Biology, The University of Texas at Arlington, Arlington, TX, USA
[e] The Amphibian and Reptile Diversity Research Center, University of Texas at Arlington, Arlington, TX, USA

ARTICLE INFO

Keywords:
Cane toad
Andes
ABC
Mito-nuclear discordance
Gene flow

ABSTRACT

The high levels of Neotropical biodiversity are commonly associated with the intense Neogene-Quaternary geological events and climate dynamics. Here, we investigate the evolutionary history of two species of Neotropical closely related amphibians (*R. horribilis* and *R. marina*). We combine published data with new mitochondrial DNA sequences and multiple nuclear markers, including 12 microsatellites. The phylogenetic analyses showed support for grouping the samples in two main clades; *R. horribilis* (Central America and Mexico) and *R. marina* (South America east of the Andes). However, the phylogenetic inferences also show an evident mito-nuclear discordance. We use Approximate Bayesian Computation (ABC) to test the role of different events in the diversification between the two groups recovered. We found that both species were affected primarily by a recent Pleistocene divergence, which was similar to the divergence estimate revealed by the Isolation-with-Migration model, under persistent bidirectional gene flow through time. We provide the first evidence that *R. horribilis* is differentiated from the South American *R. marina* at the nuclear level supporting the taxonomic status of *R. horribilis*, which has been controversial for more than a century.

1. Introduction

The Neotropics, which comprises South and Central America, the southern part of Mexico, southern Florida and Caribbean islands, is one of the most biodiverse regions of the world, where major geological, hydrological and climatic events during the Neogene and Pleistocene have traditionally been regarded as possible candidates for triggering biological diversification (e.g., Haffer, 1969; Flores-Villela and Fernández, 1994; Rull, 2011; Turchetto-Zolet et al., 2013). The emergence of a land bridge linking the two American continents (Isthmus of Panama) and the uplift of the Andes were among the most critical historical events, with pronounced biogeographic and evolutionary consequences on patterns of biodiversity at global and regional scales (Santos et al., 2009; Bacon et al., 2015). However, molecular phylogeographic studies have also emphasized Quaternary climatic changes as an important driver of diversification for Neotropical biota (e.g., Antonelli et al., 2010; Damasceno et al., 2014; Rull and Montoya, 2014). Indeed, it is well-documented that Pleistocene glacial/interglacial cycles associated with sea-level changes have introduced important modifications in habitat composition and concomitant ecological constraints that likely contributed to diversification of a wide range of Neotropical organisms (Rull, 2004, 2005, 2008; Carnaval and Moritz, 2008; Silva et al., 2019).

Despite the accumulated studies, the mechanisms behind such patterns of differentiation are still intensively debated, and traditionally have been expressed in two main but not mutually exclusive hypotheses: long-distance dispersal and vicariance (Savage, 1982; Nason et al., 2002; Mayle, 2004; Yoder and Nowak, 2006). While distinguishing between these two models of diversification is still challenging, commonly reported idiosyncratic phylogeographic patterns

* Corresponding author at: Laboratório de Evolução, Universidade Federal do Pará, Campus Universitário de Bragança, Alameda Leandro Ribeiro s/n 68, 600-000 Bragança, Pará, Brazil.
E-mail address: mvallino@ufpa.br (M. Vallinoto).

https://doi.org/10.1016/j.ympev.2019.106723
Received 22 April 2019; Received in revised form 23 December 2019; Accepted 23 December 2019
Available online 28 December 2019
1055-7903/

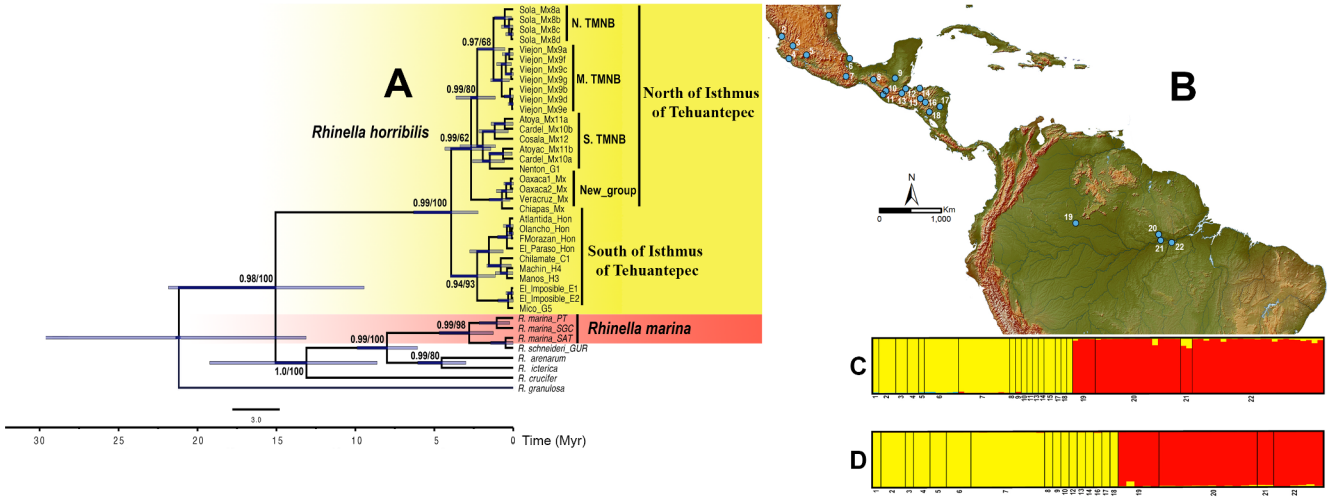

Fig. 1. (A) Mitochondrial *cyt b* gene tree as inferred by Bayesian and Maximum Likelihood analyses for *Rhinella horribilis* and *R. marina*. Bootstraps and Bayesian posterior probabilities are above branches. *Rhinella granulosa* and *R. crucifer* were used as outgroups. (B) Map of Central and South America with indication of sampling sites coded as in in Table 1 and in Table S2, Supplementary data 2. (C) Structure results (K = 2) based on haplotypes at three nuclear loci (*RPL3*, *RPL9* and *C-MYC*), and (D) on 12 microsatellite loci. Individuals are ordered by location from north to south. Individuals assigned to *R. horribilis* are indicated in yellow and *R. marina* in red. (For interpretation of the references to colour in this figure legend, the reader is referred to the web version of this article.)

among similarly distributed or co-distributed taxa show that species-specific ecological and/or life-history traits can account for different responses to shared landscape changes (Miller et al., 2008; Antonelli et al., 2010; Ornelas et al., 2013; Amei and Smith, 2014; Smith et al., 2014). For example, two recent comparative large-scale phylogeographic studies on the influence of major Neotropical paleogeological events for genetic diversification, Smith et al. (2014) and Silva et al. (2019), revealed highly discordant spatial and temporal patterns of genetic differentiation across bird lineages.

The Neotropical *Rhinella marina* species group is one of the several groups of organisms that originate either in Central America or South America, with subsequent differentiation on opposite sides of the Andean Cordillera (Patton et al., 1997; Collins and Dubach, 2000; Roberts et al., 2006; Bacon, 2013; Bacon et al., 2015; Pirie et al., 2018). This species group has a wide distribution range through South and Middle America, and it is of particular interest for testing hypotheses of diversification. Most species of this group occur across South America (Frost, 2018), with the exception of the recently revalidated *R. horribilis* (Wiegmann, 1833), which was removed from synonymy with *R. marina* by Acevedo et al. (2016) based on mitochondrial DNA and morphometric data. Following this taxonomic revision, *R. horribilis* occurs west of Andean Cordillera and as far north as the southern tip of Texas (USA), while *R. marina* occurs in the eastern part of the Andes across the entire Amazon basin. Despite the reported concordance between this phylogeographic break and the Andes mountains cordillera, their history of divergence is still not well understood and remains contentious. Indeed, the role of the Andean uplift on diversification of the *R. marina* species group is particularly puzzling because the estimated split time of east and west populations differed substantially across previous mitochondrial-based studies (Slade and Moritz, 1998; Mulcahy et al., 2006; Vallinoto et al., 2010). According to Slade and Moritz (1998), such divergence occurred at the Pliocene/Pleistocene boundary, likely associated with the uplift of the Andean Cordillera, while both Mulcahy et al. (2006) and Vallinoto et al. (2010) have suggested a relatively old split, during marine incursions and the formation of the Pebas wetland system (early Pliocene/Miocene).

According to Vallinoto et al. (2010), this large discrepancy on divergence-time estimates was likely due to differences in mtDNA mutation-rate calibration, since Slade and Moritz (1998) in their study, used a rate of evolution inferred over the whole mtDNA molecule across several vertebrate species (Wilson et al., 1985), which is substantially higher than the mutation rate reported for the specific mtDNA genes (particularly in toad species) used in the other studies of *R. marina* (Macey et al., 1998; Mulcahy and Mendelson, 2000). Nevertheless, other sources of potential errors, including coalescent stochasticity and the possibility of gene flow occurring during diversification, prevent a thorough understanding of the diversification process of *R. marina* (Edwards and Beerli, 2000; Edwards et al., 2005; Toews and Brelsford, 2012). Accounting for gene flow is of particular importance because conflicting signals between mitochondrial and nuclear-based phylogenies have been associated with interspecific hybridization involving *R. marina* and its closely related species *R. schneideri*, a widespread species from central and southern regions of South America (Sequeira et al., 2011; Vallinoto et al., 2017). By contrasting levels of differentiation at several nuclear loci and mtDNA, Sequeira et al. (2011) and Vallinoto et al. (2017) hypothesized an extensive unidirectional mtDNA introgression from *R. schneideri* into *R. marina*, suggesting that this process likely led to a complete replacement of *R. marina* mtDNA by that of *R. schneideri*. If this hypothesis is true, we expect bias toward an overestimation of time since divergence between *R. horribilis* and *R. marina* populations, since mtDNA sequences from *R. marina* populations possess *R. schneideri* mtDNA.

It is now widely accepted that combining information across multiple loci with methods that account for the uncertainties of the stochastic nature of the evolutionary process, as well as the possibility of gene flow during the process of divergence (Edwards and Beerli, 2000), is substantially improving inferences on the historical diversification of organisms (Li and Durbin, 2011; Frantz et al., 2013). Here, we apply several coalescent-based approaches under a statistical framework, including testing models of diversification based on Approximate Bayesian Computation (ABC) inference methods (e.g., Beaumont et al., 2002), and Isolation-with-Migration model (IM, Hey and Nielsen, 2004; Hey and Nielsen, 2007) to reconstruct the history of divergence between populations from west (*R. horribilis*) and east (*R. marina*) of the Andes. Using a data set consisting of two types of nuclear markers (eight nuclear gene genealogies and 12 microsatellite markers) and one mitochondrial gene, we address whether timing and pattern of diversification correspond to the uplift of the Andes or more recent climatic fluctuations of the Pleistocene after Andean formation.

Table 1
Code, taxon, locality information and sample sizes (N), and sequences downloaded from GenBank and their respective reference.

Code	Taxon	Locality	longitude	latitude	N	References
1	*R.* horribilis	La Colmena - México	98°42′23.37″W	25° 0′56.05″N	1	Present study
2	*R.* horribilis	Nayarit - México	104°50′22.29″W	21°42′46.51″N	3	Present study
3	*R.* horribilis	Jalisco - México	103°41′32.74″W	20°36′42.56″N	1	Present study
4	*R.* horribilis	Callejones - México	103°41′58.70″W	18°49′59.35″N	2	Present study
5	*R.* horribilis	Michoacán - México	103°41′32.74″W	20°36′42.56″N	2	Present study
6	*R.* horribilis	Palma Sola (Veracruz) - México	96°25′39.92″W	19°46′5.11″N	3	Present study
7	*R.* horribilis	San Pedro Ixcatlán - México	96°30′36.62″W	18° 8′39.81″N	9	Present study
8	*R.* horribilis	Pijijiapan (Chiapas) - México	93°12′38.71″W	15°41′6.19″N	1	Present study
9	*R.* horribilis	Petén - Guatemala	90°17′48.39″W	16°54′32.44″N	1	Present study
10	*R.* horribilis	Huehuetenango - Guatemala	91°30′9.24″W	15°19′58.56″N	1	Present study
11	*R.* horribilis	San Marcos - Guatemala	91°49′0.91″W	14°58′32.04″N	1	Present study
12	*R.* horribilis	Izabal - Guatemala	88°56′38.31″W	15°35′9.13″N	1	Present study
13	*R.* horribilis	Zacapa - Guatemala	89°31′57.91″W	14°58′37.06″N	1	Present study
14	*R.* horribilis	Atlántida - Honduras	7° 8′32.00″W	15°40′5.50″N	1	Present study
15	*R.* horribilis	Francisco Morazán - Honduras	87° 3′59.02″W	14°27′20.20″N	1	Present study
16	*R.* horribilis	Olancho - Honduras	85°46′15.35″W	14°48′16.89″N	1	Present study
17	*R.* horribilis	El Paraíso - Honduras	86°25′8.43″W	14° 4′21.36″N	1	Present study
18	*R.* horribilis	Matagalpa - Nicaragua	85°54′37.96″W	12°55′54.79″N	1	Present study
19	*R.* marina	S. G da Cachoeira (AM) - Brazil	67° 5′10.97″W	0° 6′39.99″S	15	Present study
20	*R.* marina	Porto Trombetas (PA) - Brazil	56°22′46.18″W	1°28′1.21″S	29	Sequeira et al. (2011) Vallinoto et al. (2017)
21	*R.* marina	Santarém (PA) - Brazil	54°43′46.97″W	2°28′18.25″S	20	Sequeira et al. (2011) Vallinoto et al. (2017)
22	*R.* marina	Juruti (PA)- Brazil	56° 5′50.73″W	2°10′1.52″S	4	Vallinoto et al. (2017)
23	*R.* horribilis	Sinaloa - México	106°42′5.37″W	24°27′21.15″N	1	Mulcahy et al. (2006)
24	*R.* horribilis	Guerrero - México	100°26′40.70″W	17°14′6.43″N	2	Mulcahy et al. (2006)
25	*R.* horribilis	Palma Sola (Veracruz)- México	96°25′39.92″W	19°46′5.11″N	4	Mulcahy et al. (2006)
26	*R.* horribilis	El Viejón (Veracruz) - México	96°36′10.20″W	19°30′38.61″N	7	Mulcahy et al. (2006)
27	*R.* horribilis	Cardel (Veracruz) - México	96°21′33.01″W	19°21′13.83″N	2	Mulcahy et al. (2006)
28	*R.* horribilis	Huehuetenango (near Nenton) - Guatemala	91°43′33.08″W	15°45′30.89″N	1	Mulcahy et al. (2006)
29	*R.* horribilis	Montanas del Mico - Guatemala	88°54′58.32″W	15°29′45.78″N	1	Mulcahy et al. (2006)
30	*R.* horribilis	Ahuachapán - EL Salvador	89°50′55.92″W	13°55′29.95″N	2	Mulcahy et al. (2006)
31	*R.* horribilis	Las Manos - Honduras	86°34′18.15″W	13°47′37.28″N	1	Mulcahy et al. (2006)
32	*R.* horribilis	Quebrada Machin - Honduras	85°20′14.94″W	15°38′39.33″N	1	Mulcahy et al. (2006)
33	*R.* horribilis	Chilamate – Costa Rica	84° 5′12.60″W	10°27′8.32″N	1	Mulcahy et al. (2006)
–	*R. schneideri*	Gurupi (TO) - Brazil	49° 4′14.12″O	11°42′43.52″S	2	Vallinoto et al. (2017)
–	*R. schneideri*	Pontalina (GO) - Brazil	49°27′44.68″O	17°31′18.63″S	6	Vallinoto et al. (2017)
–	*R. icterica*	São Paulo (SP) - Brazil	46°33′33.30″W	23° 9′51.41″S	1	Sequeira et al. (2011)
–	*R. arenarum*	Rocha - Uruguay	54°19′25.41″O	34°30′24.32″S	1	Sequeira et al. (2011)
–	*R. crucifer*	Prado (BA) - Brazil	39°13′58.39″W	17°20′17.84″S	1	Vallinoto et al. (2017)
–	*R. granulosa*	Porto Trombetas (PA) - Brazil	56°22′46.18″W	1°28′1.21″S	1	Present study

2. Material and methods

2.1. Sampling

We obtained 94 tissue samples of *R. marina* and *R. horribilis* from 33 localities (Fig. 1 and Table 1). Samples were collected through fieldwork and through loans from different herpetological collections. All tissues were preserved in 96% ethanol, and the DNA extraction was performed using the Wizard Genomic Purification Kit (PROMEGA).

2.2. Markers and protocols

We sequenced a fragment of ~409 base pairs (bp) of the mitochondrial cytochrome *b* gene (cyt *b*), and eight single-copy nuclear genealogies (*nuDNA*): ~504 bp of intron 6 of the ribosomal protein L9 gene (*RPL9*); ~675 bp of intron 5 of the ribosomal protein L3 gene (*RPL3*); ~582 bp of partial exon and intron 2 of the cellular myelocytomatosis oncogene gene (*C-MYC*); ~371 bp of intron 7 of the beta-fibrinogen gene (*fib7*); ~322 bp of the cyclin B2 gene intron 3 (*CCNB2-3*); ~283 bp of the rhodopsin gene (*Rhod1A*); ~400 bp of the seven in absentia gene (*SIA*), and; ~592 bp of the proopiomelano-cortin A gene (*POMC*). We obtained sequences of the mtDNA *cyt b* gene from 68 individuals of *R. marina* and 31 of *R. horribilis*, while the dataset constructed for the *RPL9*, *RPL3*, and *C-MYC* featured 39 individuals of *R. marina* and 30 of *R. horribilis*. Sequences of five nuDNA genes (*fib7*, *CCNB2-3*, *Rhod1A*, *SIA*, and *POMC*) were gathered for a subset of individuals from both species (five of *R. marina* and six of *R. horribilis*) for phylogenetic analysis (species tree) and reconstruction of the ancestral area (Table 1, but see below). Three species belonging to the *R. marina* species group (*R. schneideri*, *R. arenarum* and *R. icterica*) and two species closely related to that group (*Rhinella crucifer* and *R. granulosa*) were used as outgroups (Table 1). Primer information and detailed laboratory procedures employed to amplify and to sequence mtDNA and nuDNA markers are available in Table S1 (Supplementary data 1). All newly acquired sequences were deposited in GenBank under the accession numbers (Table S1; S2; S3, Supplementary data 2).

All sequences were aligned through ClustalW (Thompson et al., 1994), as implemented in GENEIOUS 9.0.5 (https://www.geneious.com). Heterozygous insertions or deletions (indels) of nuclear DNA sequences were examined in the CODONCODE ALIGNER 2.0.6 (CodonCode Corporation, Dedham, MA, USA) and through manual inspection of chromatograms. Then, we used the Bayesian algorithm PHASE 2.1.1 (Stephens and Donnelly, 2003; Stephens et al., 2001) implemented in the DNAsp 5.0 (Librado and Rozas, 2009) to infer the haplotype phases using all known phases of haplotypes. We ran PHASE three times under different random seeds and checked if haplotype estimation was consistent across runs. Each run was conducted for 10^6 iterations with the default settings.

We also used twelve microsatellite loci (RM1, RM2, RM5, RM6, RM10, RM11, M200-12, M200-11, M200-12, M200-5 M250-8 and M300-8) previously described by Bessa-Silva et al. (2015; see also Table S2 in Supplementary data 1, for details about laboratory procedures),

which were genotyped for 79 individuals (35 *R. horribilis* and 44 *R. marina,* respectively; Table S4 in Supplementary data 2). We tested all microsatellite loci for allele dropouts, stuttering and null alleles in MICRO-CHECKER 2.2.3 (Van Oosterhout et al., 2004). As MICRO-CHECKER requires larger sample sizes to assess the presence of null alleles, and because we used an individual-based sampling strategy, only locality 21 (with the largest sample size; N > 20) was used for these tests. There is no evidence of null alleles, significant allele dropouts, or stuttering identified in previous studies using these microsatellite loci (Bessa-Silva et al., 2015; Bessa-Silva et al., 2016; Vallinoto et al., 2017).

2.3. Phylogenetic analyses, structure and genetic diversity

Phylogenetic analyses were performed under Maximum Likelihood (ML) and Bayesian Inference (BI). In the case of mtDNA, we combined sequences generated in this study with those available in the literature (Mulcahy et al., 2006), producing a matrix of 39 sequences.

The maximum likelihood analyses were performed in RAxML 8.2.4 (Stamatakis, 2014), and node support was based on rapid bootstrap analyses with 1000 pseudo-replicates. We performed Bayesian analysis for the different datasets in BEAST2 2.0.3 (Bouckaert et al., 2014). We ran two independent MCMC chains of $1x10^6$ generations and parameter estimates sampling every 10,000 generations, discarding the first 10% as burn-in. We used a Yule speciation model (Drummond et al., 2006) and an uncorrelated lognormal relaxed molecular clock (Drummond et al., 2006). The resulting trees were generated using TREEANNOTATOR 2.0.3 (Bouckaert et al., 2014) and visualized in FIGTREE 1.4.3 (Rambaut et al., 2014). To select the best-fit partitioning schemes and models of evolution we used the PARTITIONFINDER 1.1.1 (Lanfear et al., 2016; Table S3 in Supplementary data 1).

For both mtDNA and nuDNA sequences (*RPL9*, *RPL3* and *C-MYC*), we calculated summary statistics in DNAsp, including the number of haplotypes (NH), nucleotide (π) and haplotype diversity (H). Genetic distance between *R. marina* and *R. horribilis* was calculated as the number of net nucleotide substitutions per site (*Da*; Nei, 1987, equation 10.21) and as the uncorrected genetic distance (p-distance) in DNAsp.

To investigate patterns of genetic structure, we first estimated the genealogical relationship among haplotypes, analysing each locus separately with a phylogenetic approach to build haplotype networks, as implemented in HAPLOVIEWER (Salzburger et al., 2011). For the construction of networks, we removed the indels because they had neither significantly reduced the number of polymorphic sites nor influenced the information in all three nuclear data sets. Patterns of genetic structure were examined in STRUCTURE 2.3.4 (Pritchard et al., 2000), based on the nuDNA sequences (*RPL9*, *RPL3*, and *C-MYC*) and microsatellites, separately. For nuDNA sequences, we first converted sequences to STRUCTURE input file format using XMFA2STRUCT (http://www.xavierdidelot.xtreemhost.com/index.htm). For both microsatellites and nuDNA sequences, we ran STRUCTURE allowing for mixed ancestry and correlated allele frequencies, with 10 independent replicates for each *K* (1–10), using 1×10^6 Markov chain Monte Carlo (MCMC) iterations, and discarding the first 5×10^4 as burn-in. The optimal number of *K* (clusters) was selected based on the highest values of the log posterior probability of the data [Ln P(D)] (Pritchard et al., 2000), and by ΔK method (Evanno et al., 2005), using the online software STRUCTURE HARVESTER 6.0 (Earl and vonHoldt, 2012). The programs CLUMPP 1.1.2 (Jakobsson and Rosenberg, 2007) and DISTRUCT 1.1 (Rosenberg, 2004) were used to align the membership coefficients of the multiple independent replicates generated by STRUCTURE and to display it graphically, respectively.

Basic statistics for microsatellites were calculated for each structure-defined cluster (*K*), including tests for departures from Hardy–Weinberg equilibrium (HWE) and linkage equilibrium (LE), observed (Ho) and expected (He) heterozygosity, and the mean number of alleles (Na) in the software ARLEQUIN 3.5 (Excoffier and Lischer, 2010). The allelic richness and private alleles richness were estimated in HP-RARE (Kalinowski, 2005), adopting the rarefaction method and hierarchical sampling to minimize the effects of unequal sample size. Genetic differentiation between structure-defined clusters as revealed by microsatellites (Weir and Cockerham, 1984) was calculated in GENODIVE 2.0b27 (Meirmans and Van Tienderen, 2004) using 999 permutations to calculate significance.

2.4. Coalescent species tree, divergence and gene flow

For species-tree inference, we used the MCMC coalescent-based Bayesian *BEAST software (Bouckaert et al., 2014), as implemented in the platform for Bayesian evolutionary analysis BEAST2 2.0.3 (Bouckaert et al., 2014). For this analysis we used the entire nuclear dataset (eight nuDNA genealogies), but we excluded the mtDNA *cyt b* to avoid the influence of mtDNA introgression between *R. schneideri* and *R. marina*, as reported by previous studies (Sequeira et al., 2011; Vallinoto et al., 2017; but see discussion section). *BEAST analysis was performed under a lognormal relaxed clock and a Yule speciation model (Drummond et al., 2006). We performed three chains of 5×10^8 steps, sampled every 5×10^4 steps, and applied a burn-in of 10%. We evaluated chain convergence with TRACER 1.6.0 (Bouckaert et al., 2014), ensuring that all ESS parameters exceeded 200. We summarized all trees using maximum clade credibility in TREEANNOTATOR 1.8.0. Substitution models were chosen with PARTITIONFINDER 2 (Lanfear et al., 2016), using BIC model selection and greedy searches (Table S3 in Supplementary data 1).

To evaluate the effects of incomplete lineage sorting (ILS) and/or gene flow as the main cause for discordance of gene trees, we applied the multispecies coalescent model (MSCM) using the R package P2C2M (Gruenstaeudl et al., 2016). This package implements a posterior predictive simulation using gene and species trees generated by *BEAST. The XML-formatted input files for *BEAST were set-up using the Python script *'BEAUTiAutomator.py'*. All simulations were performed using 100 replicates. Finally, the simulations were evaluated using the sum of test distributions from each locus using two descriptive summary statistics: *lcwt* (likelihood of the coalescent waiting times) (Reid et al., 2013) and *ndc* (number of deep coalescences) (Maddison, 1997).

Gene flow and divergence between the Central American and Mexican (*R. horribilis*) and the South American (*R. marina*) populations were estimated using the Isolation-with-Migration (IM) model implementing the IMa2 software (Hey and Nielsen, 2004; Hey, 2010). We used nuDNA *RPL9*, *RPL3* and *C-MYC* sequences together with microsatellite genotypes (12 loci) to estimate six parameters in a full IM model (two contemporary and one ancestral effective population size, divergence time, and migration rates between the two daughter populations). The stepwise-mutation model - SMM (Kimura and Ohta, 1978) was used for microsatellites, while the HKY model (Hasegawa et al., 1985) was chosen for the nuDNA genes. First, we estimated the model parameter functions through M-mode. After preliminary runs to evaluate prior settings, heated chain conditions and MCMC lengths, we estimated model parameters by using 10^6 MCMC steps, discarding 10^5 generations as burn-in. To ensure mixing of the Markov chains, we used Metropolis coupling with 100 heated chains under the geometric increment model (h1 = 0.96; h2 = 0.90). We performed two independent M-mode runs with different random seeds to check for convergence, which was assessed by monitoring values of effective sample size (ESS) > 200, trend line plots, and similarity of estimates from the first and the second half of the runs. Then, we combined sampled genealogies from each of the two independent M-mode runs to obtain the marginal posterior distribution and the maximum likelihood estimates (MLEs) of demographic parameters by running IMa2 in L-mode. Finally, we compared different demographic models using an information-theoretic approach set to phylogeographical data (Carstens et al., 2009). We applied the information theory statistics according to Burnham and Anderson (2002). To convert parameter estimates into

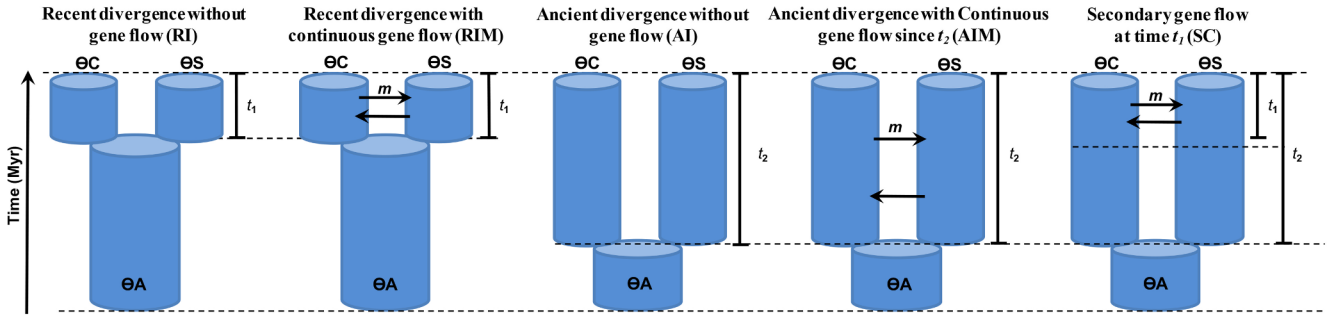

Fig. 2. Schematic representation of the five models used in the approximate Bayesian computation (ABC) analysis to infer the divergence history between *R. horribilis* and *R. marina*. Each scenario assumes a split (*t*) of an ancestral panmictic population (θA) into two daughter populations (θC and θS), with or without gene flow (*M*): (a) recent divergence without gene flow (RI); (b) recent divergence with continuous gene flow (RIM); c) ancient divergence without gene flow (AI); d) ancient divergence with continuous gene flow since divergence (AIM), and; e) Ancient divergence with secondary gene flow (SC). See Supplementary data 3 for t_1 and t_2 parameters.

demographic units we used the geometric mean of the mutation rate (4.21×10^{-6} per generation) for each nuclear locus (see Supplementary data 3 for detailed information).

2.5. Hypothesis testing by ABC coalescent simulations

We used an ABC approach to investigate the divergence history between *R. horribilis* and *R. marina*, testing concurrent scenarios that assume a subdivision of an ancestral panmictic population into two daughter populations (*R. horribilis* and *R. marina*). We tested five different scenarios (Fig. 2), which include two different times of split (t_1 and t_2) with or without gene flow (*M*), and assuming that the three populations had independent sizes that remained constant over time (N_A, N_C, and N_S): (1) Recent divergence (t_1) without gene flow (RI); (2) recent divergence (t_1) with continuous gene flow (RIM); (3) ancient divergence (t_2) without gene flow (AI); (4) ancient divergence (t_2) with continuous gene flow since divergence (AIM); (5) Ancient divergence (t_2) with secondary gene flow at time t_1 (SC). All demographic models for simulation were graphically constructed in the program POPPLANNER (Ewing et al., 2015). For each scenario we simulated $10x10^6$ datasets (3 nuDNA and 12 microsatellite loci) using the Hudson's ms program (Hudson, 2002). Following Perez et al. (2016), we calculated several summary statistics from simulated nuDNA sequence data: proportion of polymorphic sites (π), number of segregating sites (*S*), Tajima's D, Fay and Wu's *θ-H*, difference between θ_H/π-H, proportion of polymorphic sites within each population (πW) and between population (πB). We calculated the same summary statistics for the empirical data set in the *ms* simulator after the data conversion using the program FASTACONVTR (https://bioinformatics.cragenomica.es/numgenomics/people/sebas/software/software.html). For microsatellites, the genealogies were first converted to alleles in the software MICROSAT (https://www.genomicus.com/software.html), and then we used the program ARLSUMSTAT 3.5.2 (Excoffier and Lischer, 2010), a modified version of ARLEQUIN, to calculate the following summary statistics for both simulated and empirical data: number of alleles (A), expected heterozygosity (He), Garza–Williamson statistic (mN), and pairwise F_{ST} between populations (Table S1 in Supplementary data 3). A python script has been automated to perform the simulations.

We performed the ABC analysis using uniform distribution values for all parameters considered in the models (see Supplementary data 3 for more details). The only exception was the split time, for which we considered two intervals of time: t_1, recent divergence (Holocene-Pleistocene ~10,000–1,000,000 years before present) and t_2, ancient divergence ranging from t_1 (Holocene-Pleistocene) to early Pleistocene/Pliocene (t_1 – 5,000,000 years before present – see Supplementary data 3). We used a mutation rate of 4.21×10^{-6} per generation (see Supplementary data 3) and a generation time of one year (Easteal and Floyd, 1986). We evaluated the efficiency of our ABC analysis, comparing the observed and simulated data by Principal Component Analysis (Perez et al., 2016). Then, the simulated and empirical statistics were used to select the best model in the R package abc 1.4 (Csilléry et al., 2012). We also performed an estimation of parameters according to the model with the highest probability (best model) (Table 2). Finally, we used the posterior predictive check (PPC) to evaluate if the observed summary statistics remained within the posterior predictive distribution for each summary statistic based on the best model (Supplementary data 3, Table S1).

2.6. Ancestral area estimation

The historical diversification of *R. horribilis* and *R. marina* was inferred on the dated *BEAST phylogeny using the BioGeoBEARS package (Matzke, 2013, Matzke, 2014) in R v3.3.2 for Mac OS X (R Core Team). Based on the phylogeny and the occurrence areas from each species, BioGeoBEARS implements probabilistic inference of several ancestral area reconstruction models in a likelihood framework; a likelihood version of the parsimony-based Dispersal Vicariance Analysis DIVA ("DIVALIKE") model (Ronquist, 1997), the likelihood-based Dispersal-Extinction Cladogenesis (DEC) model of the LAGRANGE program (Ree et al., 2005; Ree and Smith, 2008), and the Bayesian-based BayArea ("BAYAREALIKE") model (Landis et al., 2013). BioGeoBEARS also allows testing three additional models (Matzke, 2014) incorporating the free parameter *j* (jump dispersal or founder event speciation) to any of the previously described models (DEC + J, DIVALIKE + J, and BAYAREALIKE + J). +J model assumes that individuals from a daughter lineage disperse to a new area outside the range occupied by the ancestor (Matzke, 2014, 2016a). The model that best fits the data was selected using likelihood values and Akaike Information Criterion (AIC), both implemented in the BioGeoBEARS R package (Matzke, 2013).

Table 2
Parameters estimated based on multimodels revealed by ABC from *R. horribilis* (CA) and *R. marina* (SA) based on three nuclear gene genealogies (*RLP3*, *RPL9* and *C-MYC*) and 12 microsatellite loci.

Parameters	Median	95% CI
θ_{CA}	0.7418	0.2491–1.3406
θ_{SA}	0.8237	0.0541–1.2773
τ_1	0.6701	0.4077–0.9166
$M_{CA->SA}$	3.5409	0.0928–8.3760
$M_{SA->CA}$	3.7699	0.2208–8.3882

θ = *4Neμ* (*Ne* is effective population size; *μ* is mutation rate); τ_1, divergence time (Myr); M, historical migration rate (ancestral migration between *R. marina* and *R. horribilis* in number of individuals per generation).

Table 3
Summary statistics for mtDNA cytochrome *b* and nuclear intron genes.

	N	NH	H	π
Cytb				
R. horribilis	31	20	0.9656	0.02131
R. marina	68	16	0.8670	0.01213
RPL9				
R. horribilis	28	2	0.0597	0.00012
R. marina	39	14	0.7908	0.00744
RPL3				
R. horribilis	28	4	0.1768	0.00027
R. marina	27	17	0.9338	0.00491
c-myc				
R. horribilis	30	5	0.4333	0.00153
R. marina	21	6	0.4739	0.00279

N, Number of individuals; NH, Number of haplotypes; H, haplotype diversity (expected heterozygosity using haplotypes as alleles); π, nucleotide diversity.

3. Results

3.1. Diversity and genetic variation

3.1.1. Mitochondrial DNA

A total of 36 haplotypes were found among the 99 sequences of mtDNA *cyt b* (31 sequences obtained in this study plus 68 retrieved sequences previously reported by Mulcahy et al., 2006; Sequeira et al., 2011; Vallinoto et al., 2017; Table S1, Supplementary data 2). Three haplotypes found within Central America were not previously reported (Mulcahy et al., 2006).

The haplotype network revealed two strongly differentiated groups of haplotypes separated by 37 mutations, which were geographically congruent with the ranges of *R. horribilis* (Central America and Mexico) and *R. marina* (South America east of the Andes) (Fig. S1, Supplementary data 2). Divergence between these two haplogroups was 10–11% for *Da* and *p-uncorrected*, respectively (Table S5, Supplementary data 2). Both haplogroups exhibited an overall high haplotype diversity, ranging from 0.8679 in *R. marina* to 0.9656 in *R. horribilis* (Table 3).

3.1.2. Nuclear sequence data

We sequenced three intron markers for 39 individuals of *R. marina* and 30 of *R. horribilis*. For the *RPL9* nuclear intron, we analyzed 134 sequences (39 *R. marina* and 28 *R. horribilis*). The ingroup alignment (486 bp) revealed 16 haplotypes (2 and 14 for *R. horribilis* and *R. marina*, respectively; Table 3). For *RPL3*, we analyzed 110 sequences from 55 individuals (27 *R. marina* and 28 *R. horribilis*). The ingroup alignment (664 bp) revealed 21 haplotypes (4 and 17 for *R. horribilis* and *R. marina*, respectively; Table 3). For the *C-MYC* nuclear gene, we analyzed 102 sequences from 51 individuals (21 *R. marina* and 30 *R. horribilis*). The ingroup alignment (548 bp) revealed 11 haplotypes (5 and 6 for *R. horribilis* and *R. marina*, respectively; Table 3). Mean values of both haplotype (H) and nucleotide diversity (π) were substantially higher in *R. marina* than *R. horribilis* for all nuclear markers, except for *C-MYC* (Table 3).

Results from reconstructed haplotype networks showed that none of the three nuclear loci was completely sorted with regard to *R. horribilis* and *R. marina*, albeit shared polymorphism was observed only for *C-MYC* (Fig. S1, Supplementary data 2). Also contrasting with the mtDNA results, the numbers of net nucleotide divergence (Da) between *R. marina* and *R. horribilis* were considerably reduced for all nuclear genes (less than 1%), ranging from 0.13% for *RPL3* to 0.39% for *RPL9*) (Table S5, Supplementary data 2).

3.1.3. Microsatellites

We found no evidence of null alleles, allele dropouts, or stuttering. In our analysis considering all pairs of loci, we observed no linkage disequilibrium, as well as no evidence of HWE deviations, after the correction of Bonferroni. All microsatellite loci were highly polymorphic. The average allele number per locus ranged from 3 (M300-8) to 24 (M250-8) with an average of 12.6. Genetic diversity was slightly higher in *R. marina* than *R. horribilis*. Observed and expected heterozygosity (H_O and H_E) ranged from 0.623 to 0.741, and 0.684 to 0.804, respectively for *R. horribilis* and *R. marina* (Table S6, Supplementary data 2), while allelic richness and private allelic richness ranged from 5.11 to 2.73, and 5.78 to 3.40, respectively (Table S6, Supplementary data 2).

3.2. Phylogenetic relationships and genetic structure

We conducted separate analyses of the mtDNA and nuclear DNA sequence data sets. The mtDNA-based phylogeny retrieved a similar topology to that recovered by Mulcahy et al. (2006), giving support for two main clades (Fig. 1A): one grouping all Central American and Mexican samples (*R. horribilis*), and the other comprising all samples from South America east of the Andes (*R. marina*). That is, *R. horribilis* and *R. marina* do not form a monophyletic group. This analysis also uncovered two well-supported sub-clades within the Central American and Mexican *R. horribilis clade*, which also mirrors the topology previously reported (Mulcahy et al., 2006). One of these sub-clades comprises samples mostly from north of Isthmus of Tehuantepec (NIT clade), while the other is formed by samples from south (SIT clade) of the same isthmus. Despite the two divergent groups (geographically coherent sub-clades) of haplotypes separated by the Isthmus of Tehuantepec, some samples, located south of the isthmus, are nested within the NIT clade (Chiapas2_Mx and Nenton_G1), suggesting gene flow across this potential barrier. Within the NIT clade, our analysis also shows support for the two groups previously reported by Mulcahy et al. (2006): sub-clades N. TMNB (north of the Trans-Mexico Neovolcanic Belt) / M. TMNB (middle of the Trans-Mexico Neovolcanic Belt) + S. TMNB (south of the Trans-Mexico Neovolcanic Belt). The latter includes a new sub-clade, formed by the newly uncovered haplotypes found in Oaxaca, Veracruz and Chiapas (New_group) in the present study (Fig. 1A). The divergence between NIT and SIT clades ranged from 1.5% to 3% for *Da* and *p-uncorrected* distance, respectively (Table S5, Supplementary data 2).

In contrast to the mtDNA gene tree, the *BEAST species tree analysis (combining eight nuDNA, 3728 bp) recovered *R. horribilis* and *R. marina* as a well-supported clade, and *R. schneideri* as the sister taxon of the *R. horribilis/R. marina* clade (Fig. 3). All genes show a good fit to the multispecies coalescent model (MSCM) assumptions according to the *lcwt* and *ndc* descriptive summary statistics, respectively (Table S1, supplementary data 5).

We used the Bayesian model-based clustering program STRUCTURE to detect the number of naturally occurring clusters (K) within the examined samples based on independent analysis of 12 microsatellites and three intron nuclear markers (*RPL3, RPL9* and *C-MYC*) data sets. Based on the variation of Ln P(D) and ΔK score we obtained a best-fit model of K = 2 for both data sets (Fig. S1A; B, supplementary data 4), which is consistent with the delimitation of all Central American and Mexican samples (*R. horribilis*) in one single cluster, while the second one comprises the South American (*R. marina*) samples (Fig. 1C; 1D). No further substructure was found within the Central American and Mexican cluster for both data sets (i.e. K = 3), not corroborating the levels of population structure found at mtDNA level (Fig. S2A, B, supplementary data 4). Based on microsatellites, the divergence (F_{ST}) between Central America/Mexican (*R. horribilis*) and South America east of the Andes (*R. marina*) was 0.088 (P = 0.001).

3.3. Isolation-with-migration model estimates

Based on the results recovered by *BEAST coalescent-based species tree, mtDNA and nuDNA-based phylogenetic analyses, and by the

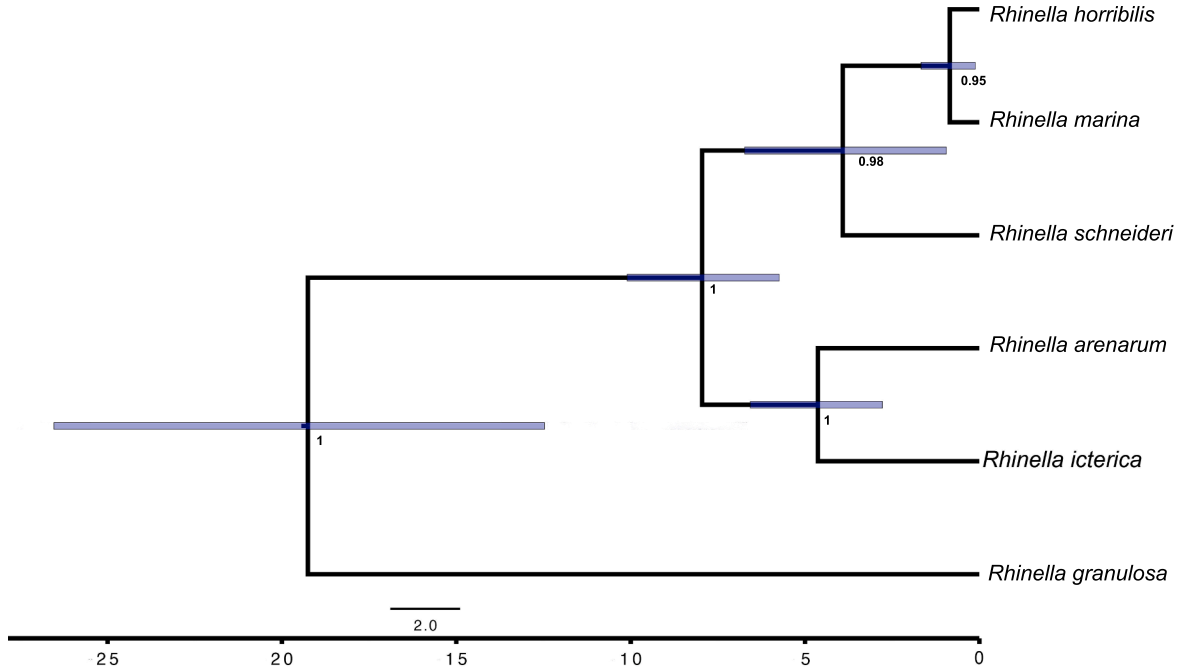

Fig. 3. Bayesian inference of species tree based on eight nuclear loci performed in *BEAST. Bayesian posterior probabilities are above branches.

Bayesian STRUCTURE analyses, we considered samples from Central America/Mexican (*R. horribilis*) and South America samples (*R. marina*), as independent units in IMa2. Then, we examined the history of divergence between these two distinct evolutionary units combining microsatellite and the three nuclear intron data sets. The respective marginal distributions are shown in Fig. S1 of supplementary data 5. The estimated divergence time between the two genetic units was ~1.033 Myr (95% HPD = 0.5325–1.758). The results showed non-zero and bidirectional and symmetric gene flow (Fig. S1, supplementary data 5). The Theta (θ) of the two daughter populations ranged from 8.600 (95% HPD = 5.400–14.20, *AC*) to 17.40 (95% HPD = 11.00–25.80, *AS*), being distinct from the ancestral population (θ_A = 2.200, 95% HPD = 1.400–3.800; Table S2, supplementary data 5). Results from likelihood ratio tests (LLR), conducted in L-mode as implemented in the IMa2 program, showed that the more complex full model is not significantly better than simpler demographic models having non-zero symmetric migration rates and populations with equal effective population size (Table S2-S3, Fig. S1, supplementary data 5).

3.4. Hypothesis testing by ABC analysis

In our preliminary simulations, the simulated summary statistics (SuSt) obtained for the original and transformed data for Principal Component Analysis (PCA) did not differ significantly in choosing the best model. In all the tests, the algorithms neural networks (NN) were considerably more efficient, showing similar posterior probabilities for original and transformed data in the choice of the best model. Thus, we set out our considerations from this algorithm. The efficiency of this analysis was also evaluated by cross-validation, which revealed a good fit of our simulations (Fig. S1, Supplementary data 3).

The results from our coalescent models showed that the scenario RIM (Recent divergence with migration in time 1 - model 2) has the highest probability (PP = 0.9527) as best model that fit our data (Fig. 2; Table S2, Supplementary data 3). Following this selected model, divergence-time estimates (t_1) fall within the Pleistocene, (t_1 = 0.6701, 95%CI: 0.4077–0.9166 Myr.) (Table 2), which was similar to the divergence estimate retrieved by IMa2.

The estimated parameter theta (θ = 4Neμ) from the selected model was similar between the Central and Mexican (0.7418; 95% CI 0.2491–1.3406) and South American populations (0.8237; 95% CI 0.0541–1.2773). Posterior predictive checks (PPC) revealed that our simulations generated ranges that cover all empirical summary statistics, suggesting a good fit of our ABC analysis (Table S1, Supplementary data 3).

3.5. Ancestral area reconstruction

All six models generated in BioGeoBEARS converged in the same biogeographical scenario, recovering South America as the most likely ancestral range of the group. In general, the "+J" models were favored over the models without founder event speciation. Besides, model comparisons showed that DIVALIKE+J model was slightly favored in

Table 4
BIOGEOBEARS model comparison between the Central America (CA) and South America (SA) lineages based on log-likelihood (lnL) and the Akaike information criterion (AIC), according to Matzke (2013, 2014). The estimated parameters include rate of dispersal (*d*); rate of extinction (*e*); founder event/jump dispersal (*j*) for Dispersal–Vicariance (DIVALIKE), Dispersal–Extinction–Cladogenesis (DEC) and Area (BAYAREALIKE) models, each of them including the parameter *j*. The final results included six models for comparison using the AIC. The best model is highlighted in bold.

Models	LnL	*np*	*d*	*e*	*j*	AIC
DEC	−7.849423	2	4.486570e-03	1.000000e-12	0.00000000	19.69885
DEC+J	−6.028227	3	1.000000e-12	1.000000e-12	0.03398817	18.05645
DIVALIKE	−7.086572	2	3.232148e-02	1.000000e-12	0.00000000	18.17314
DIVALIKE+J	**−5.220778**	**3**	**1.000000e-12**	**1.000000e-12**	**0.03056069**	**16.44156**
BAYAREALIKE	−10.647948	2	4.463301e-02	1.994647e-01	0.00000000	25.29590
BAYAREALIKE+J	−7.233784	3	1.000000e-07	1.000000e-07	0.05467807	20.46757

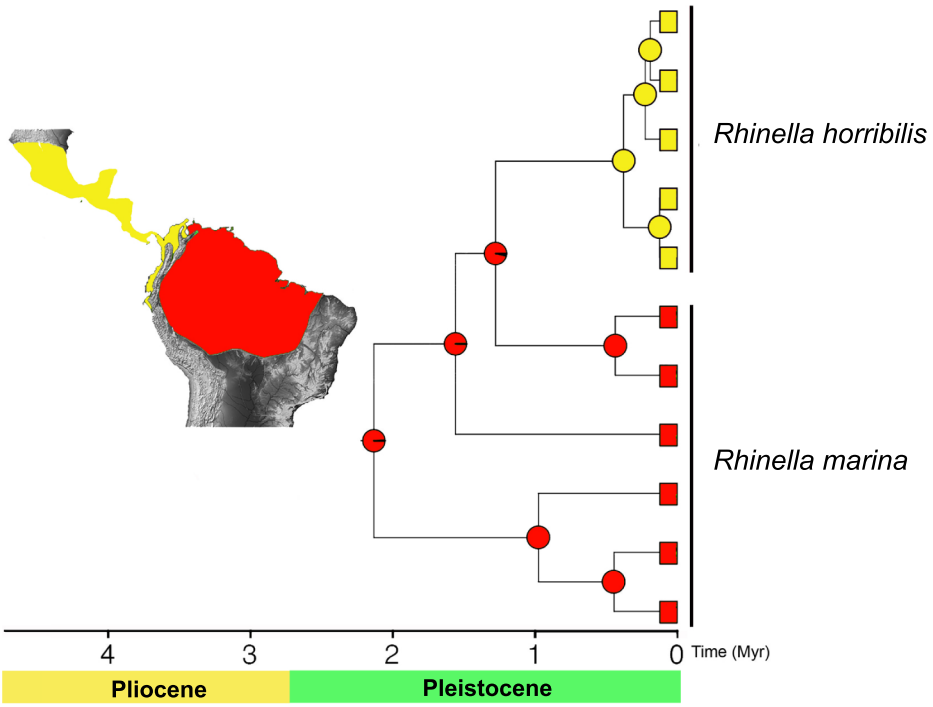

Fig. 4. Map of North, Central and South America with distribution ranges of *Rhinella horribilis* (yellow) and *R. marina* (red) (adapted from IUCN Red List, Acevedo et al. (2016) and Frost (2018)). The estimate of ancestral distributions (above nodes) for *R. horribilis* and *R. marina* using the DIVALIKE + J model (the best fitting model to the *BEAST tree and distribution ranges, see Table 4) were obtained in BioGeoBEARS. Colors represent the areas used for the biogeographical reconstructions: yellow = *R. horribilis;* red = *R. marina*. (For interpretation of the references to colour in this figure legend, the reader is referred to the web version of this article.)

terms of AIC and LnL value, being thus considered the model that best fit the data (Table 4). According to this model, vicariance, dispersion and founder events (or jump dispersal) were the major processes that gave rise to a monophyletic group that eventually dispersed westward across the Andes to occupy Central America and Mexico. Overall, the models that consider the "+J", the value of the parameters of jump dispersals (*j*) were an order of magnitude higher than rate of range-expansion dispersal (*d*).

4. Discussion

4.1. Mito-nuclear phylogenetic discordance

The present study provides, for the first time at the nuclear level, evidence for an independent evolutionary trajectory of Central American/Mexican *R. marina* populations, consistent with the recently revalidated species *R. horriblis* (Acevedo et al., 2016). The well-supported monophyly of these taxa, as recovered by the nuclear multilocus species tree, is congruent with results from Bayesian Structure clustering analyses based on both nuDNA and microsatellite markers ($K = 2$), which grouped individuals from Central America and Mexico in one single cluster. In agreement with results of nuclear data and previous molecular phylogenies, the mtDNA phylogenetic analysis also recovered *R. horribilis* as a well-supported monophyletic group. However, when we examined the position of these taxa in the broader context of the *R. marina* species group, we found marked discordance between mitochondrial and nuclear phylogenetic inferences, which raised intriguing questions on the evolutionary history of the *R. marina* group, especially regarding the divergence history between *R. horribilis* and *R. marina*. Indeed, while the phylogenetic analysis of nuclear sequence data supports a sister-taxon relationship between *R. marina* and *R. horribilis*, mtDNA-based phylogenetic analysis supports a closer relationship between *R. marina* and *R. schneideri* (two South American species).

Discordances between mtDNA and nDNA on inferring phylogenetic relationships have been intensively debated in many empirical studies and reviews (Zink and Barrowclough, 2008; Toews and Brelsford, 2012; Bonnet et al., 2017). Incomplete lineage sorting of ancestral polymorphism, introgressive hybridization or sex-biased dispersal rates are among the most common drivers of discordance in various groups. Previous multilocus phylogenetic/phylogeographic studies on the *R. marina* species complex (Sequeira et al., 2011; Vallinoto et al., 2017) revealed an extensive biogeographic mito-nuclear discordance between *R. schneideri* and *R. marina* likely caused by an ancestral hybridization. According to these authors, it is possible that the mtDNA of *R. marina* was massively introgressed or completely replaced by the mtDNA of *R. schneideri* (i.e. 'mitochondrial capture'). If this hypothesis is true, and assuming that our nuclear multilocus tree represents the true evolutionary history of the *R. marina* group, it would explain why divergence between *R. horribilis* and *R. marina* at the mitochondrial level was so much higher compared to that obtained for nuclear data (Table S5, Supplementary data 2), even accounting for differences in mutation rates between the two genomes (Nei, 2013).

Although there is a large variation in the ratio of mitochondrial over nuclear mutation rate across animals (Allio et al., 2017), in general, substitutions in mitochondrial DNA are thought to occur 5- to 20-fold faster than in nuclear DNA (Slade et al., 1994; Crawford, 2003; Johnson and Clayton, 2000; Sheldon et al., 2000). The mean ratio ($R_{mit\text{-}nu}$) of mito-nuclear divergence estimates across several species of the *R. marina* group was ≈ 7.5 (range = 6–9), with the exception of the ratio obtained for *R. horribilis/R. marina* ($R_{mit\text{-}nu}$ ≈33) and for *R. marina/R. schneideri* ($R_{mit\text{-}nu}$ ≈ 0.8), suggesting, thus, that variance in mutational rates *per se* could not be invoked to explain the mito-nuclear discordance. Furthermore, our estimated nuclear divergence time between *R. marina* and *R. schneideri* (~4.0 Myr) coincides with periods of diversification within the *R. marina* group proposed by previous studies based on either mtDNA or nuclear DNA information (Maciel et al., 2010; Vallinoto et al., 2010; Vallinoto et al., 2017). Although rigorous conclusions on the hypothesis of mtDNA capture requires further investigation, including the analysis of additional samples covering the entire range of the species, and in particular the use of model-based hypothesis-testing approaches, our reconstruction suggests that mito-nuclear phylogenetic discordance likely results from historical introgression of mtDNA between *R. marina* and *R. schneideri*.

4.2. Historical biogeography and diversification

Likelihood-based analysis of the most-probable ancestral distributional range of the *R. marina* species complex performed with BioGeoBEARS supports a South American area of original diversification (Fig. 4), suggesting that a complex model combining vicariance, dispersal and founder events (DIVALIKE + J) has promoted the diversification of this species group through the Neotropical region (Table 4). While the hypothesis of South American origin for this species group is consistent with previous findings from molecular-based inferences (Slade and Moritz, 1998; Pauly et al., 2004; Pramuk, 2006), maximum-parsimony based ancestral areas estimation (Maciel et al., 2010) and fossil records (Estes and Wassersug, 1963), the colonization of Central America and Mexico by jump dispersal or founder-event speciation process after splitting from a South American common ancestor, should be interpreted with caution. Indeed, there are some potential uncertainties in our analyses, including the lack of palaeogeographic constraints or other dispersal traits (e.g., distance, environment), and the current sampling lacks an extensive range between north of Brazil and Central America (Matzke, 2016b; Ding et al., 2019). Future work with a more comprehensive sampling and the incorporation of dispersal-related traits would be crucial to shed light on how dispersion shaped the historical biogeography of this group of toads.

Estimates of divergence time between *R. horribilis* and *R. marina* based on nuclear data yielded similar estimates using either a Bayesian coalescent time-calibrated species tree or the Isolation-with-Migration model (IMa2), ranging from 0.849 to 1.033 Ma (Fig. 3 and Table S2/ Supplementary data 5, respectively). These results suggest that these two taxa began to differentiate during the Pleistocene, after the formation of the Isthmus of Panama and the uplift of the Andes (Gregory-Wodzicki, 2000; Hoorn et al., 2010; Bacon et al., 2015; O'Dea et al., 2016), contradicting the previously inferred link between their divergence and either the chronological uplift of the Andes or occurrence of the Pebas wetland system (Moritz, 1998; Mulcahy et al., 2006; Slade and Moritz, 1998; Vallinoto et al., 2010). Yet, results from our model-based analyses supported a scenario of divergence with persistent bi-directional gene flow through time (*m* - IM and *M* – ABC, migration between *R. marina* and *R. horribilis* in number of individuals per generation) (Table 2 and Table S2-S3, Supplementary data 5), which combined with the known geographical coincidence of distributional range limits of these toad species with the Andean cordillera (Slade and Moritz, 1998; Acevedo et al., 2016), suggesting that the rise of the Andes mountains apparently did not have a direct effect on the diversification process via vicariance, but rather had indirectly acted as a porous barrier to dispersal. The hypothesis of dispersal events across the Andes, as major drivers of diversification and speciation, has been receiving increasing support from recent studies of multiple organisms for which divergence times postdating the Andean uplift, including many bird species (Miller et al., 2008; Smith et al., 2014), bats (Ditchfield, 2000; Hoffmann and Baker, 2003), bees (Dick et al., 2004), and whiteflies (Hsieh et al., 2014).

According to these studies, most cross-Andean dispersal species share some common ecological features, in particular relatively broad environmental tolerances associated with a suite of life-history traits related to high dispersal capabilities (e.g. Smith et al., 2014). In this sense, our results are somewhat intriguing regarding the commonly accepted view of amphibians as relatively poor dispersal animals with narrow eco-physiological tolerances (Ditchfield, 2000; Wells, 2010). However, there are several direct and indirect evidences suggesting that *R. marina* is not fully consistent with that view. First, *R. marina* occurs in a great variety of habitats, from tropical and subtropical forests to grasslands, savannas and xeric scrublands. Although they generally occur below 1000 m a.s.l, there are records from populations' within 1500–2200 m a.s.l along the Andean Cordillera (Barrio-Amorós, 2004; Acosta-Galvis et al., 2006). Second, available eco-physiological data from the native range suggest that *R. horribilis* (formerly *R. marina* from Middle America) has a wide temperature tolerance (Zug and Zug, 1979). Third, *R. marina* is among the world's most successful invader species, especially in Australia where it has spread rapidly, since its introduction in 1935, through western tropical and subtropical areas, and more recently through the southern temperate region (Urban et al., 2007; Jolly et al., 2016).

The occurrence of *R. marina* in more than 1.2 million km^2 of Australia, from wet tropical rainforest to xeric scrubland and cool-climate montane regions, has been at least partially linked to its broad eco-physiological tolerances (Tingley and Shine, 2011; Tingley et al., 2014; McCann et al., 2014), and extraordinarily high ability to expand into newly opened habitats (Phillips et al., 2006; Phillips et al., 2007). Indeed, recent physiological studies on locomotor performance and thermal acclimation suggested that *R. marina* is capable of rapidly shifting and adjusting its thermal tolerances to novel abiotic conditions (McCann et al., 2014; Kosmala et al., 2017). For example, McCann et al. (2014) demonstrated that *R. marina* was able to colonize cold montane areas in southeastern Australia due to its ability for rapid thermal acclimation to cooler conditions. Thus, it is possible that *R. marina*, following dynamic climatic fluctuations and associated habitat shifts during the Pleistocene, crossed the Andes throughout low/medium-elevation passes around the northern cordilleras or along the northern coast of South America (see Haffer, 1967; Dick et al., 2004). However, a more comprehensive sampling across the whole range of the species, in particular between the trans-Andean populations from the Choco region of the Pacific coast to northern Ecuador and the cis-Andean Amazonian populations, would be crucial to shed light on the process of cross-Andes and its northward continuous range expansion.

It remains difficult, with the data at hand, to establish the historical demographic contexts behind the genetic divergence of these two species. Although we found reduced genetic variability for *RPL3* and *RPL9* genes in *R. horribilis* populations compared to *R. marina,* both taxa showed broadly similar levels of genetic diversity and historical effective population sizes. These patterns are consistent with a scenario of relatively long-term diversification of *R. horribilis* populations rather than a recent process of divergence through a rapidly northward colonization (e.g., Holocene/late Pleistocene), which is often associated with a substantial loss of genetic variability across the genome (Nyström et al., 2012; Xenikoudakis et al., 2015). Furthermore, in agreement with previous results of Mulcahy et al. (2006), our data showed a marked population substructure of *R. horribilis* at the mtDNA level, which suggests that the elapsed time since the diversification of *R. horribilis* in Central America and Mexico was sufficient to accumulate genetic differentiation between conspecific populations. Indeed, the genetic discontinuity found in *R. horribilis* is broadly coincident with the Isthmus of Tehuantepec in southern Mexico, which has been considered an important biogeographic barrier causing inter- and intraspecific diversification in different groups of organisms, including amphibians (Mulcahy and Mendelson, 2000; Mulcahy et al., 2006), birds (Barber and Klicka, 2010; Rodríguez-Gómez and Ornelas, 2015), rodents (Ornelas et al., 2013) and plants (Ornelas et al., 2013). In striking contrast with mtDNA results, however, the analyses of nDNA sequence and microsatellite data sets do not reveal any geographic structuring; instead, both form a single cluster in the STRUCTURE Bayesian analysis. Incongruence of phylogeographic patterns obtained by using types of molecular markers that exhibit very different modes and rates of evolution has been commonly reported (e.g., Sequeira et al., 2008; Toews and Brelsford, 2012).

Traditional explanations for such discordances between mtDNA and nuclear markers invoked retention of ancestral polymorphism or contemporary gene flow. Compared to nuclear DNA, mtDNA exhibits faster lineage sorting due to maternal inheritance that yields a fourfold smaller effective population size than bi-parentally inherited nuclear DNA. Therefore, nuclear DNA is more likely to retain ancestral polymorphism, while mtDNA is more prone to enhance pronounced effects of genetic drift in subdivided populations (e.g., Hudson and Turelli,

2003; Zink and Barrowclough, 2008). Although we cannot rule out the possibility of extensive gene flow, given the overall lack of variation of our nuclear gene genealogies and the pattern of shared haplotypes found across all loci, the retention of ancestral polymorphism is a highly plausible explanation for such lack of population subdivision revealed by nuclear gene genealogies. In contrast with both mtDNA and nuclear gene genealogies, microsatellite markers evolve more rapidly, being particularly useful in revealing fine-scale population structure and/or inferring evolutionary processes within relatively short temporal windows (Noble, 1999; Schlötterer, 2000; Guichoux et al., 2011). The use of the same set of microsatellites in a recent phylogeographic study on *R. marina* revealed clear signs of population substructure associated with the recent historical colonization of coastal islands of the Amazon mouth in Northern Brazil (Bessa-Silva et al., 2016). On the other hand, the power of our microsatellites in unveiling two well-defined clusters corresponding to the historical divergence between *R. marina* and *R. horribilis*, suggest that homoplasy, which extensively targets microsatellites (Queney et al., 2001; Neumann et al., 2005; Sequeira et al., 2008) is highly unlikely to explain the lack of population structure.

5. Conclusions and taxonomic implications

This study provided important findings related to the long debate concerning the taxonomic status of *R. horribilis*. Until the recent revalidation of *R. horribilis* as a distinct species (Acevedo et al., 2016), its taxonomic status has been controversial for more than a century (Frost, 2018), having received the status of species or subspecies of *R. marina*, or simply being a synonym of *R. marina*. Here, we provide for the first time evidence that *R. horribilis* is differentiated of *R. marina* at the nuclear level, thus supporting an independent evolutionary trajectory of these taxa. However, regarding the relatively low divergence with the occurrence of gene flow between these taxa, even inferred from the analysis of allopatric populations only, further analysis of samples from Colombia and Venezuela near the Andes might help to elucidate the evolutionary dynamics of this system and may be critical for proper delimitation of species boundaries.

CRediT authorship contribution statement

Adam Bessa-Silva: Conceptualization, Methodology, Formal analysis, Investigation, Writing - original draft, Writing - review & editing. **Marcelo Vallinoto:** Conceptualization, Funding acquisition, Writing - original draft, Writing - review & editing. **Iracilda Sampaio:** Funding acquisition, Writing - original draft. **Oscar A. Flores-Villela:** Resources, Writing - original draft. **Eric N. Smith:** Resources, Writing - original draft. **Fernando Sequeira:** Conceptualization, Funding acquisition, Writing - original draft, Writing - review & editing.

Acknowledgments

This article is dedicated to the memories of professors Dr. Horacio Schneider and Elsen Alencar. We thank Manolo Perez for help with ABC analysis. This study was financed in part by the Coordenação de Aperfeiçoamento de Pessoal de Nível Superior - Brazil (CAPES) -Finance Code 88881.132701/2016-01 - CAPES/PDSE - n° 19/2016; and CNPq (Conselho Nacional de Desenvolvimento Científico e Tecnológico) through research project and postdoctoral grant (302892/2016-8; 422744/2018-2, 232916/2013–2016). The study was also financed by FEDER funds from the Operational Programme for Competitiveness Factors (COMPETE) and by National Funds through the Foundation for Science and Technology (FCT) under the UID/BIA/50027/2013 and POCI-01-0145-FEDER-006821 projects. Support from NSF grants DEB-0613802 and -0102383 and collecting permits in Mexico were issued by SEMARNAT to OFV. Cane toad photo provided by Nara Lins.

Appendix A. Supplementary material

Supplementary data to this article can be found online at https://doi.org/10.1016/j.ympev.2019.106723.

References

Acevedo, A.A., Lampo, M., Cipriani, R., 2016. The cane or marine toad, *Rhinella marina* (Anura, Bufonidae): two genetically and morphologically distinct species. Zootaxa 4103, 574–586.
Acosta-Galvis, A.R., Huertas-Salgado, C., Rada, M., 2006. Aproximación al conocimiento de los anfibios en una localidad del Magdalena medio (Departamento de Caldas, Colombia). Revista de la Academia Colombiana de Ciencias Exactas, Físicas y Naturales 30, 291–303.
Allio, R., Donega, S., Galtier, N., Nabholz, B., 2017. Large variation in the ratio of mitochondrial to nuclear mutation rate across animals: implications for genetic diversity and the use of mitochondrial DNA as a molecular marker. Mol. Biol. Evol. 34, 2762–2772.
Amei, A., Smith, B.T., 2014. Robust estimates of divergence times and selection with a Poisson random field model: a case study of comparative phylogeographic data. Genetics 196, 225–233.
Antonelli, A., Verola, C.F., Parisod, C., Gustafsson, A.L.S., 2010. Climate cooling promoted the expansion and radiation of a threatened group of South American orchids (Epidendroideae: Laeliinae). Biol. J. Linn. Soc. 100, 597–607.
Bacon, C., 2013. Biome evolution and biogeographical change through time. Front. Biogeogr. 5, 227–231.
Bacon, C.D., Silvestro, D., Jaramillo, C., Smith, B.T., Chakrabarty, P., Antonelli, A., 2015. Biological evidence supports an early and complex emergence of the Isthmus of Panama. Proc. Natl. Acad. Sci. 112, 6110–6115.
Barber, B., Klicka, J., 2010. Two pulses of diversification across the Isthmus of Tehuantepec in a montane Mexican bird fauna. Proc. Roy. Soc. Lond. B: Biol. Sci rspb20100343.
Barrio-Amorós, C.L., 2004. Amphibians of Venezuela systematic list, distribution and references, an update. Revista Ecología Latino Americana 9, 1–48.
Beaumont, M.A., Zhang, W., Balding, D.J., 2002. Approximate Bayesian computation in population genetics. Genetics 162, 2025–2035.
Bessa-Silva, A.R., da Cunha, D.B., Sodré, D., da Rocha, T.J., Schneider, H., Sampaio, I., Sequeira, F., Vallinoto, M., 2015. Development and characterization of microsatellite loci for *Rhinella marina* (Amphibia, Bufonidae) and their transferability to two closely related species. Conserv. Genet. Resour. 7, 247–250.
Bessa-Silva, A.R., Vallinoto, M., Sodré, D., da Cunha, D.B., Hadad, D., Asp, N.E., Sampaio, I., Schneider, H., Sequeira, F., 2016. Patterns of genetic variability in island populations of the cane toad (*Rhinella marina*) from the mouth of the Amazon. PLoS ONE 11, e0152492.
Bonnet, T., Leblois, R., Rousset, F., Crochet, P.A., 2017. A reassessment of explanations for discordant introgressions of mitochondrial and nuclear genomes. Evolution 71, 2140–2158.
Bouckaert, R., Heled, J., Kühnert, D., Vaughan, T., Wu, C.-H., Xie, D., Suchard, M.A., Rambaut, A., Drummond, A.J., 2014. BEAST 2: a software platform for Bayesian evolutionary analysis. PLoS Comput. Biol. 10, e1003537.
Burnham, K.P., Anderson, D.R., 2002. A Practical Information-Theoretic Approach. Model Selection and Multimodel Inference, second ed. Springer, New York.
Carnaval, A.C., Moritz, C., 2008. Historical climate modelling predicts patterns of current biodiversity in the Brazilian Atlantic forest. J. Biogeogr. 35, 1187–1201.
Carstens, B.C., Stoute, H.N., Reid, N.M., 2009. An information-theoretical approach to phylogeography. Mol. Ecol. 18, 4270–4282.
Collins, A., Dubach, J., 2000. Biogeographic and ecological forces responsible for speciation in Ateles. Int. J. Primatol. 21, 421–444.
Crawford, A.J., 2003. Relative rates of nucleotide substitution in frogs. J. Mol. Evol. 57, 636–641.
Csilléry, K., François, O., Blum, M.G., 2012. abc: an R package for approximate Bayesian computation (ABC). Methods Ecol. Evol. 3, 475–479.
Damasceno, R., Strangas, M.L., Carnaval, A.C., Rodrigues, M.T., Moritz, C., 2014. Revisiting the vanishing refuge model of diversification. Front. Genet. 5, 353.
Dick, C.W., Roubik, D.W., Gruber, K.F., Bermingham, E., 2004. Long-distance gene flow and cross-Andean dispersal of lowland rainforest bees (Apidae: Euglossini) revealed by comparative mitochondrial DNA phylogeography. Mol. Ecol. 13, 3775–3785.
Ding, A., Pittman, M., Upchurch, P., O'Connor, J., Field, D.J., Xu, X., 2019. The Biogeography of Coelurosaurian theropods and its impact on their evolutionary history. bioRxiv, 634170.
Ditchfield, A., 2000. The comparative phylogeography of Neotropical mammals: patterns of intraspecific mitochondrial DNA variation among bats contrasted to nonvolant small mammals. Mol. Ecol. 9, 1307–1318.
Drummond, A.J., Ho, S.Y., Phillips, M.J., Rambaut, A., 2006. Relaxed phylogenetics and dating with confidence. PLoS Biol. 4, e88.
Earl, D.A., vonHoldt, B.M., 2012. STRUCTURE HARVESTER: a website and program for visualizing STRUCTURE output and implementing the Evanno method. Conserv. Genet. Resour. 4, 359–361.
Easteal, S., Floyd, R.B., 1986. The ecological genetics of introduced populations of the giant toad, *Bufo marinus* (Amphibia: Anura): dispersal and neighbourhood size. Biol. J. Linn. Soc. 27, 17–45.
Edwards, S., Beerli, P., 2000. Perspective: gene divergence, population divergence, and the variance in coalescence time in phylogeographic studies. Evolution 54, 1839–1854.

Edwards, S.V., Kingan, S.B., Calkins, J.D., Balakrishnan, C.N., Jennings, W.B., Swanson, W.J., Sorenson, M.D., 2005. Speciation in birds: genes, geography, and sexual selection. Proc. Natl. Acad. Sci. 102, 6550–6557.
Estes, R., Wassersug, R.J., 1963. A Miocene toad from Colombia. Breviora 193, 1–13.
Evanno, G., Regnaut, S., Goudet, J., 2005. Detecting the number of clusters of individuals using the software STRUCTURE: a simulation study. Mol. Ecol. 14, 2611–2620.
Ewing, G.B., Reiff, P.A., Jensen, J.D., 2015. PopPlanner: visually constructing demographic models for simulation. Front. Genet. 6, 150.
Excoffier, L., Lischer, H.E., 2010. Arlequin suite ver 3.5: a new series of programs to perform population genetics analyses under Linux and Windows. Mol. Ecol. Resour. 10, 564–567.
Flores-Villela, O., Fernández, P.G., 1994. Biodiversidad y conservación en México: vertebrados, vegetación y uso del suelo, vol. 439, p., 2a.
Frantz, L.A., Schraiber, J.G., Madsen, O., Megens, H.-J., Bosse, M., Paudel, Y., Semiadi, G., Meijaard, E., Li, N., Crooijmans, R.P., 2013. Genome sequencing reveals fine scale diversification and reticulation history during speciation in *Sus*. Genome Biol. 14, R107.
Frost, D., 2018. Amphibian Species of the World: an Online Reference. Version 6.0. American Museum of Natural History, New York (NY), USA.
Gregory-Wodzicki, K.M., 2000. Uplift history of the Central and Northern Andes: a review. Geol. Soc. Am. Bull. 112, 1091–1105.
Gruenstaeudl, M., Reid, N.M., Wheeler, G.L., Carstens, B.C., 2016. Posterior predictive checks of coalescent models: P2C2M, an R package. Mol. Ecol. Resour. 16, 193–205.
Guichoux, E., Lagache, L., Wagner, S., Chaumeil, P., Léger, P., Lepais, O., Lepoittevin, C., Malausa, T., Revardel, E., Salin, F., 2011. Current trends in microsatellite genotyping. Mol. Ecol. Resour. 11, 591–611.
Haffer, J., 1967. Some allopatric species pairs of birds in north-western Colombia. Auk 84, 343–365.
Haffer, J., 1969. Speciation in Amazonian forest birds. Science 165, 131–137.
Hasegawa, M., Kishino, H., Yano, T.-A., 1985. Dating of the human-ape splitting by a molecular clock of mitochondrial DNA. J. Mol. Evol. 22, 160–174.
Hey, J., 2010. Isolation with migration models for more than two populations. Mol. Biol. Evol. 27, 905–920.
Hey, J., Nielsen, R., 2004. Multilocus methods for estimating population sizes, migration rates and divergence time, with applications to the divergence of *Drosophila pseudoobscura* and *D. persimilis*. Genetics 167, 747–760.
Hey, J., Nielsen, R., 2007. Integration within the Felsenstein equation for improved Markov chain Monte Carlo methods in population genetics. Proc. Natl. Acad. Sci. 104, 2785–2790.
Hoffmann, F.G., Baker, R., 2003. Comparative phylogeography of short-tailed bats (*Carollia*: Phyllostomidae). Mol. Ecol. 12, 3403–3414.
Hoorn, C., Wesselingh, F., Ter Steege, H., Bermudez, M., Mora, A., Sevink, J., Sanmartín, I., Sanchez-Meseguer, A., Anderson, C., Figueiredo, J., 2010. Amazonia through time: Andean uplift, climate change, landscape evolution, and biodiversity. Science 330, 927–931.
Hsieh, C.-H., Ko, C.-C., Chung, C.-H., Wang, H.-Y., 2014. Multilocus approach to clarify species status and the divergence history of the *Bemisia tabaci* (Hemiptera: Aleyrodidae) species complex. Mol. Phylogenet. Evol. 76, 172–180.
Hudson, R.R., 2002. Generating samples under a Wright-Fisher neutral model of genetic variation. Bioinformatics 18, 337–338.
Hudson, R.R., Turelli, M., 2003. Stochasticity overrules the "three-times rule": genetic drift, genetic draft, and coalescence times for nuclear loci versus mitochondrial DNA. Evolution 57, 182–190.
Jakobsson, M., Rosenberg, N.A., 2007. CLUMPP: a cluster matching and permutation program for dealing with label switching and multimodality in analysis of population structure. Bioinformatics 23, 1801–1806.
Johnson, K.P., Clayton, D.H., 2000. A molecular phylogeny of the dove genus *Zenaida*: mitochondrial and nuclear DNA sequences. Condor 102, 864–870.
Jolly, C.J., Shine, R., Greenlees, M.J., 2016. The impacts of a toxic invasive prey species (the cane toad, *Rhinella marina*) on a vulnerable predator (the lace monitor, *Varanus varius*). Biol. Invasions 18, 1499–1509.
Kalinowski, S.T., 2005. hp-rare 1.0: a computer program for performing rarefaction on measures of allelic richness. Mol. Ecol. Notes 5, 187–189.
Kimura, M., Ohta, T., 1978. Stepwise mutation model and distribution of allelic frequencies in a finite population. Proc. Natl. Acad. Sci. 75, 2868–2872.
Kosmala, G., Christian, K., Brown, G., Shine, R., 2017. Locomotor performance of cane toads differs between native-range and invasive populations. R. Soc. Open Sci. 4, 170517.
Landis, M.J., Matzke, N.J., Moore, B.R., Huelsenbeck, J.P., 2013. Bayesian analysis of biogeography when the number of areas is large. Syst. Biol. 62, 789–804.
Lanfear, R., Frandsen, P.B., Wright, A.M., Senfeld, T., Calcott, B., 2016. PartitionFinder 2: new methods for selecting partitioned models of evolution for molecular and morphological phylogenetic analyses. Mol. Biol. Evol. 34, 772–773.
Li, H., Durbin, R., 2011. Inference of human population history from individual whole-genome sequences. Nature 475, 493.
Librado, P., Rozas, J., 2009. DnaSP v5: a software for comprehensive analysis of DNA polymorphism data. Bioinformatics 25, 1451–1452.
Macey, J.R., Schulte II, J.A., Larson, A., Fang, Z., Wang, Y., Tuniyev, B.S., Papenfuss, T.J., 1998. Phylogenetic relationships of toads in the *Bufo bufo* species group from the Eastern Escarpment of the Tibetan Plateau: a case of vicariance and dispersal. Mol. Phylogenet. Evol. 9, 80–87.
Maciel, N.M., Collevatti, R.G., Colli, G.R., Schwartz, E.F., 2010. Late Miocene diversification and phylogenetic relationships of the huge toads in the *Rhinella marina* (Linnaeus, 1758) species group (Anura: Bufonidae). Mol. Phylogenet. Evol. 57, 787–797.
Maddison, W.P., 1997. Gene trees in species trees. Syst. Biol. 46, 523–536.
Matzke, N.J., 2013. BioGeoBEARS: BioGeography with Bayesian (and likelihood) evolutionary analysis in R Scripts. R package, version 0.2 1, 2013.
Matzke, N.J., 2014. Model selection in historical biogeography reveals that founder-event speciation is a crucial process in island clades. Syst. Biol. 63, 951–970.
Matzke, N.J., 2016a. 'BioGeoBEARS deals with "Founder-event speciation" not "founder-effect speciation." PhyloWiki essay, 2016-08-07. http://phylo.wikidot.com/biogeobears-deals-with-founder-event-speciation-not-founder.
Matzke, N.J., 2016b. Stochastic mapping under biogeographical models. PhyloWiki BioGeoBEARS website.
Mayle, F.E., 2004. Assessment of the Neotropical dry forest refugia hypothesis in the light of palaeoecological data and vegetation model simulations. J. Quat. Sci. 19, 713–720.
McCann, S., Greenlees, M.J., Newell, D., Shine, R., 2014. Rapid acclimation to cold allows the cane toad to invade montane areas within its Australian range. Funct. Ecol. 28, 1166–1174.
Meirmans, P.G., Van Tienderen, P.H., 2004. GENOTYPE and GENODIVE: two programs for the analysis of genetic diversity of asexual organisms. Mol. Ecol. Notes 4, 792–794.
Miller, M.J., Bermingham, E., Klicka, J., Escalante, P., Do Amaral, F.S.R., Weir, J.T., Winker, K., 2008. Out of Amazonia again and again: episodic crossing of the Andes promotes diversification in a lowland forest flycatcher. Proc. Roy. Soc. B: Biol. Sci. 275, 1133–1142.
Mulcahy, D.G., Mendelson III, J.R., 2000. Phylogeography and speciation of the morphologically variable, widespread species *Bufo valliceps*, based on molecular evidence from mtDNA. Mol. Phylogenet. Evol. 17, 173–189.
Mulcahy, D.G., Morrill, B.H., Mendelson III, J.R., 2006. Historical biogeography of lowland species of toads (*Bufo*) across the Trans-Mexican Neovolcanic Belt and the Isthmus of Tehuantepec. J. Biogeogr. 33, 1889–1904.
Nason, J.D., Hamrick, J., Fleming, T.H., 2002. Historical vicariance and postglacial colonization effects on the evolution of genetic structure in *Lophocereus*, a Sonoran Desert columnar cactus. Evolution 56, 2214–2226.
Nei, M., 1987. Molecular Evolutionary Genetics. Columbia University Press, New York.
Nei, M., 2013. Mutation-driven evolution. OUP Oxford.
Neumann, K., Michaux, J., Maak, S., Jansman, H., Kayser, A., Mundt, G., Gattermann, R., 2005. Genetic spatial structure of European common hamsters (*Cricetus cricetus*) - a result of repeated range expansion and demographic bottlenecks. Mol. Ecol. 14, 1473–1483.
Noble, L., 1999. Microsatellites - evolution and applications. Heredity 83, 633–634.
Nyström, V., Humphrey, J., Skoglund, P., McKEOWN, N.J., Vartanyan, S., Shaw, P.W., Lidén, K., Jakobsson, M., Barnes, I., Angerbjörn, A., 2012. Microsatellite genotyping reveals end-Pleistocene decline in mammoth autosomal genetic variation. Mol. Ecol. 21, 3391–3402.
O'Dea, A., Lessios, H.A., Coates, A.G., Eytan, R.I., Restrepo-Moreno, S.A., Cione, A.L., Collins, L.S., de Queiroz, A., Farris, D.W., Norris, R.D., 2016. Formation of the Isthmus of Panama. Sci. Adv. 2, e1600883.
Ornelas, J.F., Sosa, V., Soltis, D.E., Daza, J.M., González, C., Soltis, P.S., Gutiérrez-Rodríguez, C., De los Monteros, A.E., Castoe, T.A., Bell, C., 2013. Comparative phylogeographic analyses illustrate the complex evolutionary history of threatened cloud forests of northern Mesoamerica. PLoS ONE 8, e56283.
Patton, J., Da Silva, M., Lara, M., Mustrangi, M., 1997. Diversity, Differentiation, and the Historical Biogeography of Nonvolant Small Mammals of The Neotropical Forests. Tropical Forest Remnants: Ecology, Management, and Conservation Of Fragmented Communities. University of Chicago Press, Chicago, Illinois, pp. 455–465.
Pauly, G.B., Hillis, D.M., Cannatella, D.C., 2004. The history of a Nearctic colonization: molecular phylogenetics and biogeography of the Nearctic toads (*Bufo*). Evolution 58, 2517–2535.
Perez, M., Bonatelli, I., Moraes, E., Carstens, B., 2016. Model-based analysis supports interglacial refugia over long-dispersal events in the diversification of two South American cactus species. Heredity 116, 550.
Phillips, B.L., Brown, G.P., Greenlees, M., Webb, J.K., Shine, R., 2007. Rapid expansion of the cane toad (*Bufo marinus*) invasion front in tropical Australia. Austral Ecol. 32, 169–176.
Phillips, B.L., Brown, G.P., Webb, J.K., Shine, R., 2006. Invasion and the evolution of speed in toads. Nature 439, 803.
Pirie, M.D., Maas, P.J., Wilschut, R.A., Melchers-Sharrott, H., Chatrou, L.W., 2018. Parallel diversifications of Cremastosperma and Mosannona (Annonaceae), tropical rainforest trees tracking Neogene upheaval of South America. R. Soc. Open Sci. 5, 171561.
Pramuk, J.B., 2006. Phylogeny of south American *Bufo* (Anura: Bufonidae) inferred from combined evidence. Zool. J. Linn. Soc. 146, 407–452.
Pritchard, J.K., Stephens, M., Donnelly, P., 2000. Inference of population structure using multilocus genotype data. Genetics 155, 945–959.
Queney, G., Ferrand, N., Weiss, S., Mougel, F., Monnerot, M., 2001. Stationary distributions of microsatellite loci between divergent population groups of the European rabbit (*Oryctolagus cuniculus*). Mol. Biol. Evol. 18, 2169–2178.
Rambaut, A., Suchard, M.A., Xie, D., Drummond, A.J., 2014. Tracer v1.6, Available from http://beast.bio.ed.ac.uk/Tracer.
Ree, R.H., Moore, B.R., Webb, C.O., Donoghue, M.J., 2005. A likelihood framework for inferring the evolution of geographic range on phylogenetic trees. Evolution 59, 2299–2311.
Ree, R.H., Smith, S.A., 2008. Lagrange: software for likelihood analysis of geographic range evolution. Syst. Biol. 57, 4–14.
Reid, N.M., Hird, S.M., Brown, J.M., Pelletier, T.A., McVay, J.D., Satler, J.D., Carstens, B.C., 2013. Poor fit to the multispecies coalescent is widely detectable in empirical data. Syst. Biol. 63, 322–333.
Roberts, J.L., Brown, J.L., von May, R., Arizabal, W., Schulte, R., Summers, K., 2006. Genetic divergence and speciation in lowland and montane Peruvian poison frogs.

Mol. Phylogenet. Evol. 41, 149–164.
Rodríguez-Gómez, F., Ornelas, J.F., 2015. At the passing gate: past introgression in the process of species formation between *Amazilia violiceps* and *A. viridifrons* hummingbirds along the Mexican Transition Zone. J. Biogeogr. 42, 1305–1318.
Ronquist, F., 1997. Dispersal-vicariance analysis: a new approach to the quantification of historical biogeography. Syst. Biol. 46, 195–203.
Rosenberg, N.A., 2004. DISTRUCT: a program for the graphical display of population structure. Mol. Ecol. Notes 4, 137–138.
Rull, V., 2004. Biogeography of the 'Lost World': a palaeoecological perspective. Earth Sci. Rev. 67, 125–137.
Rull, V., 2005. Biotic diversification in the Guayana Highlands: a proposal. J. Biogeogr. 32, 921–927.
Rull, V., 2008. Speciation timing and Neotropical biodiversity: the Tertiary-Quaternary debate in the light of molecular phylogenetic evidence. Mol. Ecol. 17, 2722–2729.
Rull, V., 2011. Neotropical biodiversity: timing and potential drivers. Trends Ecol. Evol. 26, 508–513.
Rull, V., Montoya, E., 2014. *Mauritia flexuosa* palm swamp communities: natural or human-made? A palynological study of the Gran Sabana region (northern South America) within a Neotropical context. Quat. Sci. Rev. 99, 17–33.
Salzburger, W., Ewing, G.B., Von Haeseler, A., 2011. The performance of phylogenetic algorithms in estimating haplotype genealogies with migration. Mol. Ecol. 20, 1952–1963.
Santos, J.C., Coloma, L.A., Summers, K., Caldwell, J.P., Ree, R., Cannatella, D.C., 2009. Amazonian amphibian diversity is primarily derived from late Miocene Andean lineages. PLoS Biol. 7, e1000056.
Savage, J.M., 1982. The enigma of the Central American herpetofauna: dispersals or vicariance? El enigma de la herpetofauna centroamericana: dispersión o vicariancia? Ann. Mo. Bot. Gard. 69, 464–547.
Schlötterer, C., 2000. Evolutionary dynamics of microsatellite DNA. Chromosoma 109, 365–371.
Silva, S.M., Peterson, A.T., Carneiro, L., Burlamaqui, T.C.T., Ribas, C.C., Sousa-Neves, T., Batista, R., et al., 2019. A dynamic continental moisture gradient drove Amazonian bird diversification. Sci. Adv. 5, eaat5752.
Sequeira, F., Alexandrino, J., Weiss, S., Ferrand, N., 2008. Documenting the advantages and limitations of different classes of molecular markers in a well-established phylogeographic context: lessons from the Iberian endemic Golden-striped salamander, *Chioglossa lusitanica* (Caudata: Salamandridae). Biol. J. Linn. Soc. 95, 371–387.
Sequeira, F., Sodré, D., Ferrand, N., Bernardi, J.A., Sampaio, I., Schneider, H., Vallinoto, M., 2011. Hybridization and massive mtDNA unidirectional introgression between the closely related Neotropical toads *Rhinella marina* and *R. schneideri* inferred from mtDNA and nuclear markers. BMC Evol. Biol. 11, 264.
Sheldon, F.H., Jones, C.E., McCracken, K.G., 2000. Relative patterns and rates of evolution in heron nuclear and mitochondrial DNA. Mol. Biol. Evol. 17, 437–450.
Slade, R., Moritz, C., 1998. Phylogeography of *Bufo marinus* from its natural and introduced ranges. Proc. R. Soc. Lond. B Biol. Sci. 265, 769–777.
Slade, R.W., Moritz, C., Heideman, A., 1994. Multiple nuclear-gene phylogenies: application to pinnipeds and comparison with a mitochondrial DNA gene phylogeny. Mol. Biol. Evol. 11, 341–356.
Smith, B.T., McCormack, J.E., Cuervo, A.M., Hickerson, M.J., Aleixo, A., Cadena, C.D., Pérez-Emán, J., Burney, C.W., Xie, X., Harvey, M.G., 2014. The drivers of tropical speciation. Nature 515, 406.
Stamatakis, A., 2014. RAxML version 8: a tool for phylogenetic analysis and post-analysis of large phylogenies. Bioinformatics 30, 1312–1313.
Stephens, M., Donnelly, P., 2003. A comparison of Bayesian methods for haplotype reconstruction from population genotype data. Am. J. Hum. Genet. 73, 1162–1169.
Stephens, M., Smith, N.J., Donnelly, P., 2001. A new statistical method for haplotype reconstruction from population data. Am. J. Hum. Genet. 68, 978–989.
Thompson, J.D., Higgins, D.G., Gibson, T.J., 1994. CLUSTAL W: improving the sensitivity of progressive multiple sequence alignment through sequence weighting, position-specific gap penalties and weight matrix choice. Nucleic Acids Res. 22, 4673–4680.
Tingley, R., Shine, R., 2011. Desiccation risk drives the spatial ecology of an invasive anuran (*Rhinella marina*) in the Australian semi-desert. PLoS ONE 6, e25979.
Tingley, R., Vallinoto, M., Sequeira, F., Kearney, M.R., 2014. Realized niche shift during a global biological invasion. Proc. Natl. Acad. Sci. 201405766.
Toews, D.P., Brelsford, A., 2012. The biogeography of mitochondrial and nuclear discordance in animals. Mol. Ecol. 21, 3907–3930.
Turchetto-Zolet, A., Pinheiro, F., Salgueiro, F., Palma-Silva, C., 2013. Phylogeographical patterns shed light on evolutionary process in South America. Mol. Ecol. 22, 1193–1213.
Urban, M.C., Phillips, B.L., Skelly, D.K., Shine, R., 2007. The cane toad's (*Chaunus* [*Bufo*] *marinus*) increasing ability to invade Australia is revealed by a dynamically updated range model. Proc. Roy. Soc. Lond. B: Biol. Sci. 274, 1413–1419.
Vallinoto, M., Cunha, D.B., Bessa-Silva, A., Sodré, D., Sequeira, F., 2017. Deep divergence and hybridization among sympatric Neotropical toads. Zool. J. Linn. Soc. 180, 647–660.
Vallinoto, M., Sequeira, F., Sodré, D., Bernardi, J.A., Sampaio, I., Schneider, H., 2010. Phylogeny and biogeography of the *Rhinella marina* species complex (Amphibia, Bufonidae) revisited: implications for Neotropical diversification hypotheses. Zoolog. Scr. 39, 128–140.
Van Oosterhout, C., Hutchinson, W.F., Wills, D.P., Shipley, P., 2004. MICRO-CHECKER: software for identifying and correcting genotyping errors in microsatellite data. Mol. Ecol. Notes 4, 535–538.
Weir, B.S., Cockerham, C.C., 1984. Estimating F-statistics for the analysis of population structure. Evolution 38, 1358–1370.
Wells, K.D., 2010. The Ecology and Behavior of Amphibians. University of Chicago Press.
Wilson, A.C., Cann, R.L., Carr, S.M., George, M., Gyllensten, U.B., Helm-Bychowski, K.M., Higuchi, R.G., Palumbi, S.R., Prager, E.M., Sage, R.D., 1985. Mitochondrial DNA and two perspectives on evolutionary genetics. Biol. J. Linn. Soc. 26, 375–400.
Xenikoudakis, G., Ersmark, E., Tison, J.L., Waits, L., Kindberg, J., Swenson, J.E., Dalén, L., 2015. Consequences of a demographic bottleneck on genetic structure and variation in the Scandinavian brown bear. Mol. Ecol. 24, 3441–3454.
Yoder, A.D., Nowak, M.D., 2006. Has vicariance or dispersal been the predominant biogeographic force in Madagascar? Only time will tell. Annu. Rev. Ecol. Evol. Syst. 37, 405–431.
Zink, R.M., Barrowclough, G.F., 2008. Mitochondrial DNA under siege in avian phylogeography. Mol. Ecol. 17, 2107–2121.
Zug, G.R., Zug, P.B., 1979. The marine toad, *Bufo marinus*: a natural history resume of native populations. Smithsonian Contribut. Zool. 284, 1–58.